

This is a repository copy of *A Gold(I)–Acetylene Complex Synthesised using Single-Crystal Reactivity*.

White Rose Research Online URL for this paper:

<https://eprints.whiterose.ac.uk/212252/>

Version: Published Version

Article:

Weller, Andrew orcid.org/0000-0003-1646-8081, Johnson, Chloe-Louise, Gyton, Matthew Robert orcid.org/0000-0002-7565-5154 et al. (1 more author) (2024) *A Gold(I)–Acetylene Complex Synthesised using Single-Crystal Reactivity*. *Angewandte Chemie International Edition*. e202404264. ISSN 1433-7851

<https://doi.org/10.1002/anie.202404264>

Reuse

This article is distributed under the terms of the Creative Commons Attribution (CC BY) licence. This licence allows you to distribute, remix, tweak, and build upon the work, even commercially, as long as you credit the authors for the original work. More information and the full terms of the licence here:

<https://creativecommons.org/licenses/>

Takedown

If you consider content in White Rose Research Online to be in breach of UK law, please notify us by emailing eprints@whiterose.ac.uk including the URL of the record and the reason for the withdrawal request.



A Gold(I)–Acetylene Complex Synthesised using Single-Crystal Reactivity

Chloe L. Johnson, Daniel J. Storm, M. Arif Sajjad, Matthew R. Gyton, Simon B. Duckett,*
 Stuart A. Macgregor,* Andrew S. Weller,* Miquel Navarro,* and Jesús Campos*

Abstract: Using single-crystal to single-crystal solid/gas reactivity the gold(I) acetylene complex $[\text{Au}(\mathbf{L1})(\eta^2\text{-HC}\equiv\text{CH})][\text{BAR}^{\text{F}}_4]$ is cleanly synthesized by addition of acetylene gas to single crystals of $[\text{Au}(\mathbf{L1})(\text{CO})][\text{BAR}^{\text{F}}_4]$ [$\mathbf{L1}$ = tris-2-(4,4'-di-tert-butylbiphenyl)phosphine, $\text{Ar}^{\text{F}} = 3,5\text{-(CF}_3)_2\text{C}_6\text{H}_3$]. This simplest gold-alkyne complex has been characterized by single crystal X-ray diffraction, solution and solid-state NMR spectroscopy and periodic DFT. Bonding of $\text{HC}\equiv\text{CH}$ with $[\text{Au}(\mathbf{L1})]^+$ comprises both σ -donation and π -backdonation with additional dispersion interactions within the cavity-shaped phosphine.

Acetylene, $\text{HC}\equiv\text{CH}$, is the simplest of all alkynes, and an important chemical feedstock due to its availability and high reactivity.^[1] Despite this, transition metal catalyzed transformations of acetylene are relatively underdeveloped.^[2] While cationic gold(I) complexes, exemplified by $[\text{Au}(\text{L})]^+$ (L = phosphine or NHC), have been shown to be powerful, and tuneable, catalytic systems for the electrophilic activation of substituted alkynes,^[3] their use with acetylene is limited to recent reports by Echavarren, who demonstrated its use as a C_2 -building block in aryloxyvinylolation or cyclopropanation reactions.^[4] In such transformations π -acetylene gold(I) intermediates are postulated, but their isolation or

even spectroscopic detection remains elusive. This contrasts with the well-developed coordination chemistry of gold(I) alkyne adducts more generally.^[5] Additional interest in π -acetylene adducts of d^{10} coinage metals stems from the fundamental insight they provide into metal-ligand bonding, especially the role of back-donation from their filled d-orbitals to the π -ligand.^[6] However, synthetically, such studies are restricted to a handful examples of isolated Cu and Ag-complexes, with no Au-examples known, and none of which are of direct relevance to the cationic $[\text{Au}(\text{L})]^+$ systems so popular in catalysis (Figure 1A).^[6b,7] For example the group of Dias recently described a set of π -acetylene complexes of silver and copper, but the isolation of analogous gold(I) complexes was unsuccessful due to rapid decomposition.^[8]

We have recently reported on the use of sterically demanding terphenyl phosphine ligands, with $\text{PMe}_2(\text{C}_6\text{H}_3\text{-}2,6\text{-(C}_6\text{H}_3\text{-}2',6'\text{-Pr}_2)_2)$ as our archetypal example, to synthesize otherwise unstable gold(I) complexes through kinetic stabilization, for instance hydrocarbyl-bridged cationic digold complexes.^[9] However these phosphine complexes did not provide access to π -acetylene adducts, whose formation could only be postulated during acetylene activation by Au-based bimetallic frustrated Lewis pairs.^[10] In contrast the even bulkier, cavity-shaped, ligand tris-2-(4,4'-di-tert-butylbiphenyl)phosphine, $\mathbf{L1}$ (Figure 1B), does allow for the isolation of the dicoordinate gold(I) ethylene complex, $[\text{Au}(\mathbf{L1})(\eta^2\text{-H}_2\text{C}=\text{CH}_2)][\text{SbF}_6]$, $\mathbf{1}[\text{SbF}_6]$, and its reaction with CO to form $[\text{Au}(\mathbf{L1})(\text{CO})][\text{SbF}_6]$, $\mathbf{2}[\text{SbF}_6]$, Figure 1B.^[11] We now describe the use of this ligand in the synthesis, isolation and characterization of a gold(I) π -acetylene adduct. Notably this complex is best accessed by sequential single-crystal *in crystallo*^[12] ligand exchange reactions (Figure 1C).

Informed by the synthesis of the ethene adduct, $\mathbf{1}[\text{SbF}_6]$,^[11a] the reaction of $\text{Au}(\mathbf{L1})\text{Cl}$ with the halide-abstracting agent $\text{Ag}[\text{SbF}_6]$ was undertaken in CH_2Cl_2 solution (298 K, 1 hr) in the presence of excess acetylene (1.5 bara, bara = bar absolute). However, rather than forming a gold(I) π -acetylene complex, only unidentified decomposition products were observed. The addition of acetylene (1.5 bara) to CD_2Cl_2 solutions of $\mathbf{1}[\text{SbF}_6]$ or $\mathbf{2}[\text{SbF}_6]$ was also investigated. However, all attempts to make the target acetylene adduct using these complexes resulted in only partial conversion of the starting materials, and decomposition on removal of the acetylene atmosphere under vacuum, to give a black precipitate of gold(0) and free phosphine, $\mathbf{L1}$.

Recognizing the now well-established role counterions play in the reactivity and stability of cationic gold(I)

[*] C. L. Johnson, Dr. M. R. Gyton, Prof. S. B. Duckett, Prof. A. S. Weller
 Department of Chemistry, University of York, York, YO10 5DD, UK
 E-mail: andrew.weller@york.ac.uk
 simon.duckett@york.ac.uk

D. J. Storm, Dr. M. A. Sajjad, Prof. S. A. Macgregor
 EaSTCHEM School of Chemistry, University of St Andrews, North
 Haugh, St Andrews, KY16 9ST, UK
 E-mail: sam38@st-andrews.ac.uk

Dr. M. Navarro, Dr. J. Campos
 Instituto de Investigaciones Químicas (IIQ), Departamento de
 Química Inorgánica and Centro de Innovación en Química
 Avanzada (ORFEO-CINQA)
 Consejo Superior de Investigaciones Científicas (CSIC) and Uni-
 versity of Sevilla, 41092 Sevilla, Spain
 E-mail: miquel.navarro@uam.es
 jesus.campos@iiq.csic.es

© 2024 The Authors. Angewandte Chemie International Edition published by Wiley-VCH GmbH. This is an open access article under the terms of the Creative Commons Attribution License, which permits use, distribution and reproduction in any medium, provided the original work is properly cited.

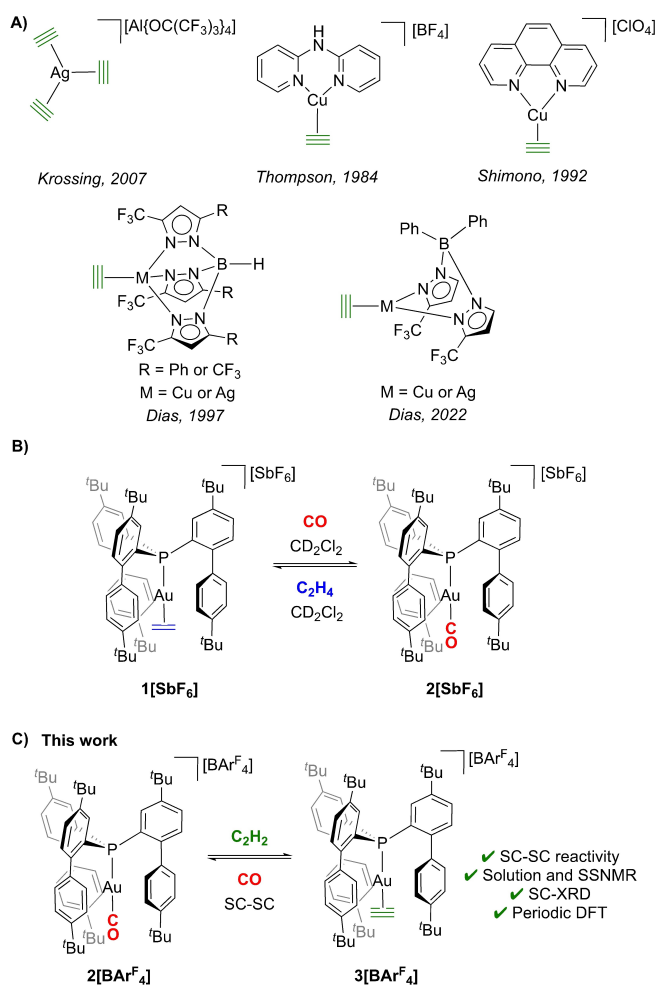


Figure 1. A) Examples of structurally-characterized d^{10} acetylene complexes. B) Ligand exchange at $[\text{Au}(\text{L1})(\eta^2\text{-H}_2\text{C}=\text{CH}_2)][\text{SbF}_6]$, **1** $[\text{SbF}_6]$. C) Access to stable gold acetylene adduct $[\text{Au}(\text{L1})(\eta^2\text{-HC}\equiv\text{CH})][\text{BAR}^{\text{F}}_4]$, **3** $[\text{BAR}^{\text{F}}_4]$, using solid/gas SC-SC reactivity (SC-SC = single-crystal to single-crystal).

complexes,^[3b] the anion $[\text{SbF}_6]^-$ was swapped for the less-coordinating $[\text{BAR}^{\text{F}}_4]^-$ anion $[\text{Ar}^{\text{F}} = 3,5\text{-(CF}_3)_2\text{C}_6\text{H}_3]$ (Supporting Materials) to form the corresponding ethene **1** $[\text{BAR}^{\text{F}}_4]$, and CO **2** $[\text{BAR}^{\text{F}}_4]$, adducts. Charging **1** $[\text{BAR}^{\text{F}}_4]$ with acetylene (1.5 bara) resulted in 85 % conversion to form a new complex, while full conversion was obtained using **2** $[\text{BAR}^{\text{F}}_4]$. This new species was assigned to the acetylene adduct $[\text{Au}(\text{L1})(\eta^2\text{-HC}\equiv\text{CH})][\text{BAR}^{\text{F}}_4]$, **3** $[\text{BAR}^{\text{F}}_4]$, by in situ NMR spectroscopy. However, definitive characterisation of pure **3** $[\text{BAR}^{\text{F}}_4]$ in the absence of acetylene (and its associated acetone carrier solvent) was hindered by decomposition (~20 %) on the application of a dynamic vacuum to the solution.

In crystallo^[12] solid-state molecular organometallic chemistry (SMOM)^[13] has emerged as a useful methodology to access solution-unstable organometallic species by single-crystal to single-crystal (SC-SC) reactivity, for example cationic group 9 σ -alkane complexes.^[14] For such cationic species, the periodic arrangement of $[\text{BAR}^{\text{F}}_4]^-$ anions in the lattice has been shown to provide a well-defined micro-

environment where non-covalent interactions provide stabilization,^[15] while substrate-accessible hydrophobic channels allow for solid/gas reactivity.^[16] Given the solution-based substitution chemistry noted above to generate **3** $[\text{BAR}^{\text{F}}_4]$ we hypothesized that solid/gas SC-SC reactivity could be used to isolate this gold(I) acetylene complex in a pure form without the decomposition observed using solution routes.

Crystals of the starting material **1** $[\text{BAR}^{\text{F}}_4]$ were therefore grown from 1,2-difluorobenzene/heptane solution. Visual inspection revealed them to be colourless blocks, that exist in two different polymorphs for **1** $[\text{BAR}^{\text{F}}_4]$, having space groups $P2_1/n$ (**1** $[\text{BAR}^{\text{F}}_4]$) and $P\bar{1}$ (**1** $[\text{BAR}^{\text{F}}_4]$). Both phases are susceptible to solvent loss, however crystals of **1** $[\text{BAR}^{\text{F}}_4]$ are particularly sensitive under an extended argon purge, resulting in multiply faceted crystals which do not diffract. Both polymorphs show the same cation structure, within error, and motif of $[\text{BAR}^{\text{F}}_4]^-$ anions, but show a variation in the lattice solvent of crystallization. We restrict a detailed discussion to **1** $[\text{BAR}^{\text{F}}_4]$. A single crystal X-ray diffraction (SCXRD) study of **1** $[\text{BAR}^{\text{F}}_4]$ reveals a structure for the $[\text{Au}(\text{L1})(\eta^2\text{-H}_2\text{C}=\text{CH}_2)]^+$ cation very similar to that reported for **1** $[\text{SbF}_6]$,^[11a] Figure 2A. Notably, the C=C double bond of 1.199(6) Å [150 K] is shorter than in free ethylene [1.313 Å].^[17] Previously this was suggested to be due to minimal backbonding from the cationic d^{10} center. While this may be the case, an additional interpretation is that the ethene shows torsional libration^[6b,18] in the solid-state that artificially shortens the measured C...C distance. Support for this comes from the fact that the C...C bond appears to shorten at higher data collection temperatures [1.302(5) Å, 100 K; 1.199(6) Å, 150 K; 1.089(9) Å, 200 K; 1.04(1) Å, 250 K] as the amplitude of alkene libration increases. The $[\text{BAR}^{\text{F}}_4]^-$ anions form a biccapped square prismatic packing

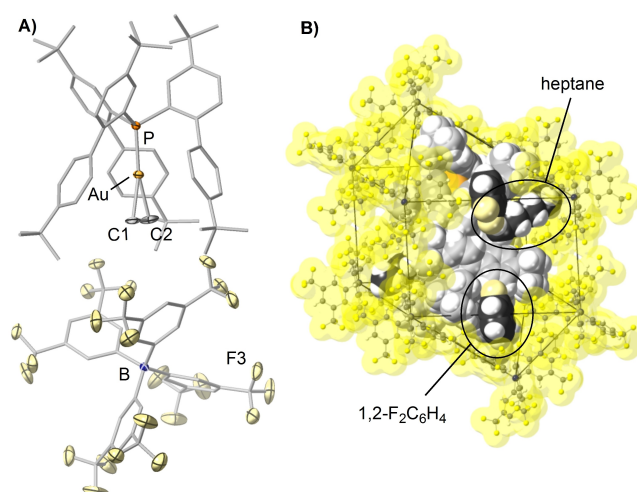
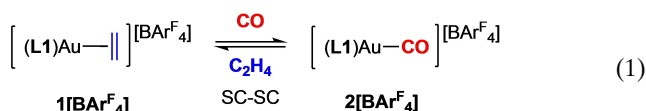


Figure 2. (A) Molecular representation of solution-grown crystals of **1** $[\text{BAR}^{\text{F}}_4]$, showing the relationship between the cation and a proximal $[\text{BAR}^{\text{F}}_4]^-$ anion. Displacement ellipsoids shown at 50% probability. Hydrogen atoms are excluded for clarity. (B) Packing diagram of **1** $[\text{BAR}^{\text{F}}_4]$ (van der Waals radii), with solvent of crystallization highlighted.

motif, with two crystallographically identical cations of $\mathbf{1}^+$ enclosed by 10 anions (Figure 2B). 1,2-F₂C₆H₄ (0.9 occupancy) and heptane (0.75 occupancy) are fractionally occupied within the lattice of polymorph $\mathbf{1}'[\text{BAr}^{\text{F}}_4]$, while $\mathbf{1}[\text{BAr}^{\text{F}}_4]$, has only heptane incorporated into its lattice.

This ensemble of $\mathbf{1}[\text{BAr}^{\text{F}}_4]$ and $\mathbf{1}'[\text{BAr}^{\text{F}}_4]$ was characterized by solution (CD₂Cl₂) and solid-state NMR spectroscopy (SS NMR). The former shows the [Au(L1)(η^2 -H₂C=CH₂)]⁺ cation to be essentially unchanged from that reported for $\mathbf{1}[\text{SbF}_6]$.^[11a] A broad signal at δ 109.4 is observed in the ¹³C{¹H} SS NMR spectrum for bound ethene. Consistent with two polymorphs, in the ³¹P{¹H} SS NMR spectrum two environments are observed at δ 16.5 and 11.7. No significant coupling to quadrupolar ¹⁹⁷Au ($I=3/2$) nucleus is observed.^[19]



Addition of CO (4 bara, 10 min) to the ensemble of crystalline $\mathbf{1}[\text{BAr}^{\text{F}}_4]/\mathbf{1}'[\text{BAr}^{\text{F}}_4]$ results in the complete conversion to $\mathbf{2}[\text{BAr}^{\text{F}}_4]/\mathbf{2}'[\text{BAr}^{\text{F}}_4]$ as measured by SCXRD, ³¹P{¹H}/¹³C{¹H} SS NMR spectroscopy, infrared (IR) spectroscopy and solution (CD₂Cl₂) NMR of the dissolved product, Equation 1. The ¹³C{¹H} SS NMR spectrum shows a doublet corresponding to the Au(CO) group at δ 182.0 [²J_{CP} = 110 Hz] and an absence of the ethene signal at δ 109.4. In the IR spectrum $\nu(\text{CO})=2170 \text{ cm}^{-1}$.^[20] Analysis by SCXRD (space group = $P\bar{1}$) of $\mathbf{2}[\text{BAr}^{\text{F}}_4]$ shows the cation is very similar to $\mathbf{2}[\text{SbF}_6]$, Figure 3.^[11a] The arrangement of [BAr^F₄]⁻ anions, and the lattice solvent, are retained from $\mathbf{1}[\text{BAr}^{\text{F}}_4]$. This reaction is reversible, and on addition of ethene

(2 bara) to crystals of $\mathbf{2}[\text{BAr}^{\text{F}}_4]$ full conversion to $\mathbf{1}[\text{BAr}^{\text{F}}_4]$ is observed.

Addition of acetylene (1.5 bara, 30 mins) to crystals of the ensembles of polymorphs of $\mathbf{1}[\text{BAr}^{\text{F}}_4]$, or $\mathbf{2}[\text{BAr}^{\text{F}}_4]$, resulted in the formation of the gold π -acetylene complex $\mathbf{3}[\text{BAr}^{\text{F}}_4]$, as determined by solution ³¹P{¹H} NMR spectroscopy of the dissolved crystals. However, full conversion to $\mathbf{3}[\text{BAr}^{\text{F}}_4]$ was only observed from the CO-complex $\mathbf{2}[\text{BAr}^{\text{F}}_4]$ in these solid/gas reactions, as measured by solution and solid-state NMR, SCXRD and IR spectroscopy. In the ¹H NMR spectrum of dissolved crystalline material (CD₂Cl₂) a new doublet was observed at δ 2.02 [³J_{HP} = 2.6 Hz] this is assigned to the bound acetylene, which collapses to a singlet on decoupling ³¹P. The corresponding acetylene peak was observed as a doublet at δ 76.0 [²J_{CP} = 9 Hz] in the ¹³C{¹H} NMR spectrum (Figure 4), while a single resonance is recorded in the ³¹P{¹H} NMR spectrum (δ 8.9). These spectroscopic markers are consistent with a bound acetylene at an {AuP} fragment;^[21] i.e. [Au(L1)(η^2 -HC≡CH)] [BAr^F₄], $\mathbf{3}[\text{BAr}^{\text{F}}_4]$. These signals are shifted slightly to higher frequency than those of free acetylene [¹H: δ 1.80, ¹³C{¹H}: δ 71.9].^[8] In the corresponding ¹³C{¹H} SS NMR spectrum two broad signals (fwhm ~ 35 Hz) are observed at δ 76.3 and 75.2 for the acetylene in the two polymorphs; while two environments are observed at δ 10.2, 8.0 in the ³¹P{¹H} SS NMR spectrum.

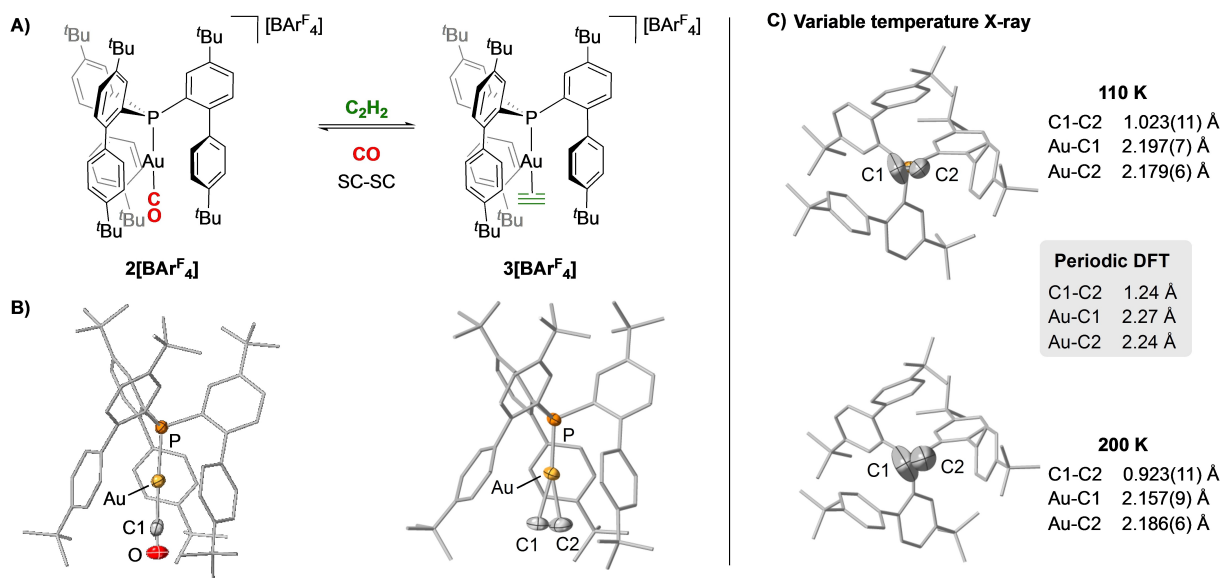
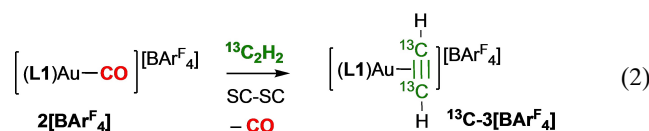


Figure 3. (A) Synthesis of $\mathbf{3}[\text{BAr}^{\text{F}}_4]$. (B) Molecular structures of solution-grown crystals of the cations $\mathbf{2}^+$ and $\mathbf{3}^+$ (110 K collection). Displacement ellipsoids shown at 50% probability. All hydrogen atoms, [BAr^F₄]⁻ and lattice solvent are excluded for clarity. Selected bond lengths (Å): $\mathbf{2}[\text{BAr}^{\text{F}}_4]$, C1–O, 1.058(8); Au–C1, 2.001(6); Au–P, 2.3002(11); $\mathbf{3}[\text{BAr}^{\text{F}}_4]$, Au–P, 2.2747(7). (C) Alternative representation of $\mathbf{3}^+$ showing the torsional disorder at 110 K and 200 K data collection temperatures, highlighting the acetylene ADPs and key structural metrics. Calculated distances from Periodic DFT.

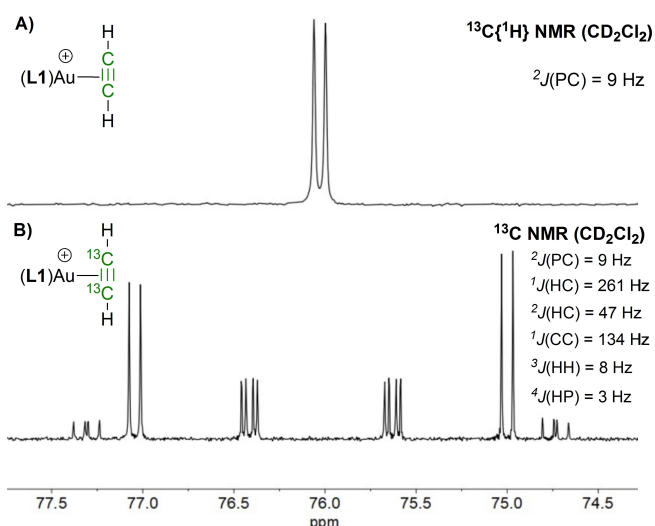


Figure 4. Acetylene region of ^{13}C NMR (A) $^{13}\text{C}\{^1\text{H}\}$ NMR spectrum $3[\text{BAr}^{\text{F}}_4]$ (298 K, CD_2Cl_2). (B) ^{13}C NMR spectrum $3[\text{BAr}^{\text{F}}_4]$ (298 K, CD_2Cl_2). (C) ^{13}C NMR spectrum $^{13}\text{C}-3[\text{BAr}^{\text{F}}_4]$ (298 K, CD_2Cl_2).

By using doubly ^{13}C labelled acetylene gas, the isotopologue $[\text{Au}(\text{L1})(\eta^2\text{-H}^{13}\text{C}\equiv^{13}\text{CH})][\text{BAr}^{\text{F}}_4]$, $^{13}\text{C}-3[\text{BAr}^{\text{F}}_4]$, was synthesized using the same solid/gas SC-SC route (Equation 2). In the resulting solution ^1H and ^{13}C NMR spectra signals for an AA'MM'X spin system for bound acetylene are observed, that were successfully simulated using gNMR (Supporting Materials).^[22] Figure 4 shows the ^{13}C NMR spectrum. The $^1J(\text{CC})$ value was determined to be 134 Hz, which is considerably lower than that of free acetylene, 172 Hz.^[23] $^1J(\text{CH})$ and $^2J(\text{CH})$ values are 261 and 47 Hz respectively, the former being larger than for free acetylene (248 and 47 Hz respectively),^[24,25] and considerably larger than for other acetylene complexes.^[26]

The formation of $3[\text{BAr}^{\text{F}}_4]$ arises from two sequential SC-SC solid/gas transformations, that result in some crystal-degradation. This meant that although a gross structure could be obtained for the cation from a SCXRD experiment, the precise location of the acetylene could not be determined, likely due to the torsional vibration of bound acetylene (vide infra). Importantly, unlike in solution, in the crystalline phase $3[\text{BAr}^{\text{F}}_4]$ does not lose acetylene under extended vacuum (72 hrs, 10^{-2} mbar), although single-crystallinity is lost, along with lattice heptane (NMR).^[27] This chemical stability allows for subsequent recrystallization of $3[\text{BAr}^{\text{F}}_4]$ from 1,2-difluorobenzene/heptane to give high quality single-crystalline materials in which the acetylene ligand is now better defined. Screening these block-like crystals again revealed the existence of two different polymorphs, and both provided good quality diffraction data, allowing for two independent structural solutions of the gold(I)-acetylene complex to be collected. $3[\text{BAr}^{\text{F}}_4]$ crystallizes in space group $P2_1/n$, and $3'[\text{BAr}^{\text{F}}_4]$ in $P\bar{1}$. Both show the bicapped square prismatic motif of $[\text{BAr}^{\text{F}}_4]^-$ anions with 1,2- $\text{F}_2\text{C}_6\text{H}_4$ lattice solvent, but only the latter also has heptane incorporated into the lattice. Both cations offer very similar structural metrics (Supporting

Materials), and only $3[\text{BAr}^{\text{F}}_4]$ is discussed in detail. The $^{31}\text{P}\{^1\text{H}\}$ and $^{13}\text{C}\{^1\text{H}\}$ SS NMR data of this ensemble are essentially identical to those obtained by direct SC-SC reactivity. This reaction is reversible, and addition of CO to crystalline $3[\text{BAr}^{\text{F}}_4]$ regenerates $2[\text{BAr}^{\text{F}}_4]$. These are rare examples of sequential single-crystal to single-crystal solid/gas transformations with gold complexes, although topotactic transformations are known,^[28] as well as solid/gas transformations on Cu(I) and Ag(I) systems.^[29]

Figure 3 shows that the gold(I) centre adopts a linear coordination geometry, with the acetylene ligand bound in an η^2 -fashion. Similar to $1[\text{BAr}^{\text{F}}_4]$, the $\text{C}\equiv\text{C}$ triple bond [1.023(11) Å, collected at 110 K] appears artificially shorter than that of free acetylene [1.2033(2) Å],^[30] a result of torsional vibrations. Similar behaviour has been discussed in detail for silver and copper acetylene adducts.^[8] Consistent with this, there is a trend for the $\text{C}\equiv\text{C}$ bond to appear shorter at higher data collection temperatures: 1.023(11) Å, 110 K; 0.980(9) Å, 150 K; 0.923(11) Å, 200 K (Figure 3C), although within error these distances are the same. The ADPs for C1 and C2, and trend in $\text{Au}\cdots\text{C}$ distances, suggest a torsional pivot around $\text{Au}-\text{C}2$. At the lowest collection temperature (110 K) the $\text{Au}\cdots\text{C}$ distances are apparently shorter [2.197(7), 2.179(6) Å] than reported for the related gold(I) alkyne complex $[\text{Au}(\text{P}^i\text{Bu}_3)(\eta^2\text{-MeC}\equiv\text{C}^i\text{Bu})][\text{SbF}_6]$ where no such disorder is reported: 2.238(12), 2.239(10) Å.^[21] Thus while the structure shows gold/acetylene binding, the metrical data do not allow for a detailed analysis of bonding. Using the empirical correlation proposed by Dias,^[8] a weak IR band for the $\text{C}\equiv\text{C}$ stretch that is observed at 1656 cm^{-1} , shifted 318 cm^{-1} from free acetylene (1974 cm^{-1}), provides an estimated $\text{C}\equiv\text{C}$ distance of 1.27 Å. This $\text{C}\equiv\text{C}$ stretch compares with those reported for the d^{10} complexes $(\text{R}_2\text{PC}_2\text{H}_4\text{PR}_2)\text{Pd}(\eta^2\text{-HC}\equiv\text{CH})$, R^iBu , 1626 cm^{-1} ; R^iPr , 1619 cm^{-1} .^[26] The acetylene $\text{C}-\text{H}$ stretch in $3[\text{BAr}^{\text{F}}_4]$ is observed at 3185 cm^{-1} . This band shifts to 3175 cm^{-1} in the isotopologue $^{13}\text{C}-3[\text{BAr}^{\text{F}}_4]$ (calculated 3176 cm^{-1}); while the $^{13}\text{C}\equiv^{13}\text{C}$ stretch is no longer observed (calculated 1592 cm^{-1}) due to masking by the broad $\text{C}-\text{H}$ vibration of **L1** at 1611 cm^{-1} .

To resolve the torsional disorder seen crystallographically the structure of $3[\text{BAr}^{\text{F}}_4]$ was fully optimised in the solid state using periodic DFT. This gave a $\text{C}\equiv\text{C}$ distance of 1.24 Å, while retaining asymmetric $\text{Au}-\text{C}$ distances ($\text{Au}-\text{C}1=2.27\text{ Å}$; $\text{Au}-\text{C}2=2.24\text{ Å}$, see Figure 3C). This behaviour is also seen in calculations on the isolated cation and is therefore not a solid state effect, but reflects the C_2H_2 orientation within the binding pocket provided by the **L1** ligand, with $\text{C}2-\text{H}2$ pointing directly at one aryl substituent and $\text{C}1-\text{H}1$ directed between the other two.

An ETS-NOCV analysis on the optimised 3^+ cation built from L1Au^+ and C_2H_2 fragments gives an interaction energy of -41.3 kcal/mol , made up of destabilising steric interactions ($+22.9\text{ kcal/mol}$) and stabilizing orbital (-57.6 kcal/mol) and dispersion interactions (-6.6 kcal/mol). The key orbital interactions are displayed as deformation density channels in Figure 5. The major component is alkyne σ -donation to a $\text{Au}-\text{P}$ σ^* -acceptor that is dominated by $\text{Au}(6s)$ character (58.4%; $\Delta E=-28.3\text{ kcal/mol}$). This is

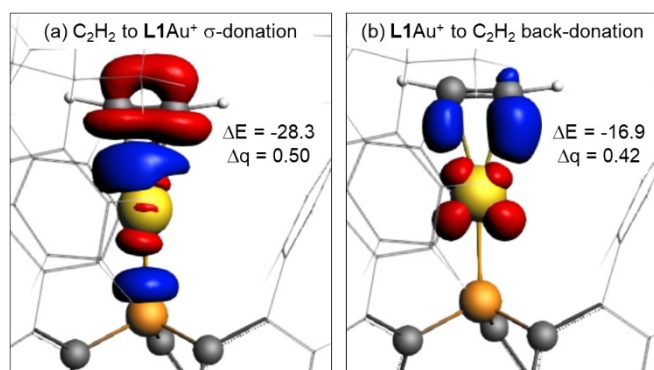


Figure 5. Major ETS-NOCV deformation density channels (isovalue 0.003 au) for the $L1Au^+-C_2H_2$ interaction in 3^+ . Charge flow (Δq) from red to blue with energies in kcal/mol. Key atoms: ball and stick; ligand substituents: wire frame.

supplemented by Au(5d) to alkyne $\pi^*_{||}$ donation (-16.9 kcal/mol), consistent with previous calculations showing π -back donation^[31] from Au(I) can be significant. Repeating this analysis with a truncated model where the appended p - t Bu- C_6H_4 substituents are replaced by H gives a lower interaction energy of -35.8 kcal/mol. This reduction reflects a lower dispersion contribution (-1.2 kcal/mol) indicating that the full **L1** binding pocket does confer some added stability on C_2H_2 binding. The presence of weak interactions between the alkyne and the surrounding ligand environment was confirmed by QAIM, NCI and IGMH studies (see Supporting Materials).

In summary, we have synthesized and structurally characterized the first gold(I)-acetylene complex, $[Au(L1)(\eta^2-HC\equiv CH)][BAR^F_4]$ ($3[BAR^F_4]$; **L1** = tris-2-(4,4'-di-tert-butylbiphenyl)phosphine). This simplest alkyne complex has been characterized by variable temperature single crystal X-ray diffraction, solution and solid-state NMR spectroscopy, including the use of doubly ^{13}C labelled acetylene gas and periodic DFT. The synthesis of $3[BAR^F_4]$, that provides structural and spectroscopic markers for the coordination of acetylene in Au(I)-mediated catalysis, hinges on the synergistic interplay of two pivotal factors: ligand confinement and *in crystallo* solid/gas reactivity. Firstly, the use of the cavity-shaped phosphine **L1** establishes a confined environment that imparts enhanced stability to the Au-bound acetylene through steric protection within the binding pocket, as well as some further stabilizing weak interactions for the C_2H_2 fragment. An ETS-NOCV analysis identifies σ -donation from the alkyne to gold as the primary bonding interaction, that is supplemented by substantial π -back-donation. Secondly, the isolation of $3[BAR^F_4]$ in pure form was made possible only through single-crystal to single-crystal (SC-SC) reactivity. This represents a further illustration of the potential of solid-state molecular organometallic chemistry (SMOM) for isolating complexes that are unstable in solution.

Acknowledgements

This work was supported by the European Research Council (ERC Starting Grant, CoopCat, Project 756575) and the Spanish Ministry of Science and Innovation (PID2022-139782NB-I00). M. N. acknowledges the Spanish Ministry of Science and Innovation and Junta de Andalucía for post-doctoral programs (FJC2018-035514-I and DOC_00149). Leverhulme Trust (RPG-2020-184; MRG, CLJ) and the Wild Overseas Scholar's Fund (CLJ); the University of St. Andrews (DJS) and EPSRC (EP/W015498/1, MAS; UK Catalysis Hub, EP/R026815/1, MRG). Dr A. Whitwood (York) for helpful discussions and Dr V. Annis (York) for technical assistance with ^{13}C -acetylene experiments. This work used the ARCHER2 UK National Supercomputing Service (<https://www.archer2.ac.uk>).

Conflict of Interest

The authors declare no conflict of interest.

Data Availability Statement

The data that support the findings of this study are available in the supplementary material of this article.

Keywords: acetylene · gold(I) · bulky phosphine · single crystals · solid-state organometallic · ligand cavity · X-ray diffraction

- [1] a) I.-T. Trotus, T. Zimmermann, F. Schütch, *Chem. Rev.* **2014**, *114*, 1761–1782; b) H. Schobert, *Chem. Rev.* **2014**, *114*, 1734–1760; c) M. S. Ledovskaya, V. V. Voronin, K. S. Rodygin, V. P. Ananikov, *Synthesis* **2022**, *54*, 999–1042.
- [2] a) R. J. Tedeschi, *Acetylene-Based Chemical from Coal and Other Natural Resources*, Dekker: New York **1982**; p 232; b) V. V. Voronin, M. S. Ledovskaya, A. S. Bogachenkov, K. S. Rodygin, P. V. Ananikov, *Molecules* **2018**, *23*, 2442–2526; c) M. S. Ledovskaya, V. V. Voronin, K. S. Rodygin, *Russ. Chem. Rev.* **2018**, *87*, 167–191; d) K. S. Rodygin, M. S. Ledovskaya, V. V. Voronin, K. Lotsman, V. P. Ananikov, *Eur. J. Org. Chem.* **2021**, *2021*, 43–52; e) B. Yang, S. Lu, Y. Wang, S. Zhu, *Nat. Commun.* **2022**, *13*, 1858–1870; f) L. Lin, B. Liu, Y. Wang, S. Li, S. Zhu, *Chem. Sci.* **2023**, *14*, 1012–1918; g) T. G. Back, K. R. Muralidharan, *J. Org. Chem.* **1991**, *56*, 2781–2787; h) H. Diaz Velazquez, Z.-H. Wu, M. Vandichel, F. Verpoort, *Catal. Lett.* **2017**, *147*, 463–471; i) D. Parasar, T. T. Ponduru, A. Noonikara-Poyil, N. B. Jayaratna, H. V. R. Dias, *Dalton Trans.* **2019**, *48*, 15782–15794; j) T. Bruhm, A. Abram, J. Häusler, O. Thomys, K. Köhler, *Chem. Eur. J.* **2021**, *27*, 16834–16839.
- [3] a) A. Leyva-Pérez, A. Corma, *Angew. Chem. Int. Ed.* **2012**, *51*, 614–635; b) Z. Lu, T. Li, S. R. Mudshinge, B. Xu, G. B. Hammond, *Chem. Rev.* **2021**, *121*, 8452–8477; c) C. M. Hendrich, K. Sekine, T. Koshikawa, K. Tanaka, A. S. K. Hashmi, *Chem. Rev.* **2021**, *121*, 9113–9163; d) I. Stylianakis, A. Koloouris, *Catalysts* **2023**, *13*, 921.
- [4] a) D. Scharnagel, I. Escofet, H. Armengol-Relats, M. E. de Orbe, J. N. Korber, A. M. Echavarren, *Angew. Chem. Int. Ed.* **2020**, *49*, 4888–4891; b) T. Medina-Gil, A. Sadurní, L. A.

- Hammarback, A. M. Echavarren, *ACS Catal.* **2023**, *13*, 10751–10755.
- [5] a) H. V. R. Dias, J. A. Flores, J. Wu, P. Kroll, *J. Am. Chem. Soc.* **2009**, *131*, 11249–11255; b) H. Schmidbaur, A. Schier, *Organometallics* **2010**, *29*, 2–23; c) T. J. Brown, R. A. Widenhoefer, *Organometallics* **2012**, *30*, 6003–6009; d) M. A. Celik, C. Dash, V. A. K. Adiraju, A. Das, M. Yousufuddin, G. Frenking, H. V. R. Dias, *Inorg. Chem.* **2013**, *52*, 729–742; e) M. Navarro, A. Toledo, S. Mallet-Ladeira, E. D. Sosa-Carrizo, K. Miqueu, D. Bourissou, *Chem. Sci.* **2020**, *11*, 2750–2758; f) M. Navarro, D. Bourissou, *Adv. Organomet. Chem.* **2021**, *76*, 101–144; g) J. Mehara, B. T. Watson, A. Noonikara-Poyil, A. O. Zacharias, J. Roithova, H. V. R. Dias, *Chem. Eur. J.* **2022**, *28*, e202103984.
- [6] a) D. J. Gorin, F. D. Toste, *Nature* **2007**, *446*, 395–403; b) A. Reisinger, N. Trapp, I. Krossing, S. Almannshofer, V. Hertz, M. Presnitz, W. Scherer, *Angew. Chem. Int. Ed.* **2007**, *46*, 8295–8298.
- [7] a) J. S. Thompson, J. F. Whitney, *Inorg. Chem.* **1984**, *23*, 2813–2819; b) M. Munakata, S. Kitagawa, I. Kawada, M. Maekawa, H. Shimono, *J. Chem. Soc. Dalton Trans.* **1992**, 2225–2230; c) H. V. R. Dias, Z. Wang, W. Jin, *Inorg. Chem.* **1997**, *36*, 6205–6215; d) A. Noonikara-Poyil, A. Munoz-Castro, H. V. R. Dias, *Molecules* **2022**, *27*, 16.
- [8] A. Noonikara-Poyil, S. G. Ridlen, I. Fernández, H. V. R. Dias, *Chem. Sci.* **2022**, *13*, 7190–7203.
- [9] a) M. F. Espada, J. Campos, J. López-Serrano, M. L. Poveda, E. Carmona, *Angew. Chem. Int. Ed.* **2015**, *54*, 15379–15348; b) J. Miranda-Pizarro, Z. Luo, J. J. Moreno, D. A. Dickie, J. Campos, B. Gunnoe, *J. Am. Chem. Soc.* **2021**, *143*, 2509–2522.
- [10] a) J. Campos, *J. Am. Chem. Soc.* **2017**, *139*, 2944–2947; b) N. Hidalgo, J. J. Moreno, M. Pérez-Jiménez, C. Maya, J. López-Serrano, J. Campos, *Organometallics* **2020**, *39*, 2534–2544.
- [11] a) M. Navarro, J. Miranda-Pizarro, J. J. Moreno, C. Navarro-Gilbert, I. Fernández, J. Campos, *Chem. Commun.* **2021**, 57, 9280–9283; b) M. Navarro, M. G. Alférez, M. de Sousa, J. Miranda-Pizarro, J. Campos, *ACS Catal.* **2022**, *12*, 4227–4241.
- [12] K. A. Reid, D. C. Powers, *Chem. Commun.* **2021**, 57, 4993–5003.
- [13] F. M. Chadwick, A. I. McKay, A. J. Martínez-Martínez, N. H. Rees, T. Krämer, S. A. Macgregor, A. S. Weller, *Chem. Sci.* **2017**, *8*, 6014–6029.
- [14] a) S. D. Pike, T. Krämer, N. H. Rees, S. A. Macgregor, A. S. Weller, *Organometallics* **2015**, *34*, 1487–1497; b) S. D. Pike, A. L. Thompson, A. G. Algarra, D. C. Apperley, S. A. Macgregor, A. S. Weller, *Science* **2012**, *337*, 1648–1651; c) A. J. Bukvic, A. L. Burnage, G. J. Tizzard, A. J. Martínez-Martínez, A. I. McKay, N. H. Rees, B. E. Tegner, T. Krämer, H. Fish, M. R. Warren, S. J. Coles, S. A. Macgregor, A. S. Weller, *J. Am. Chem. Soc.* **2021**, *143*, 5106–5120; d) C. G. Royle, L. Sotorrios, M. R. Gyton, C. N. Brodie, A. L. Burnage, S. K. Furfari, A. Marini, M. R. Warren, S. A. Macgregor, A. S. Weller, *Organometallics* **2022**, *14*, 3270–3280.
- [15] M. A. Sajjad, S. A. Macgregor, A. S. Weller, *Faraday Discuss.* **2023**, *244*, 222–240.
- [16] A. J. Martínez-Martínez, D. H. Rees, A. S. Weller, *Angew. Chem. Int. Ed.* **2019**, *58*, 16873–16877.
- [17] G. J. H. Nes, A. Vos, *Acta Crystallogr. Sect. B* **1979**, *35*, 2593.
- [18] J. Harada, K. Ogawa, S. Tomoda, *J. Am. Chem. Soc.* **1995**, *117*, 4476–4478.
- [19] K. Angermair, G. A. Bowmaker, E. N. de Silva, P. C. Healy, B. E. Jones, H. Schmidbaur, *J. Chem. Soc. Dalton Trans.* **1996**, 3121–3121.
- [20] This value is relatively higher than free CO ($\nu(\text{CO}) = 2143 \text{ cm}^{-1}$) but slightly lower to related cationic NHC (2197 cm^{-1}) and phosphine (2185 cm^{-1}) Au(I)–CO complexes: a) H. V. R. Dias, C. Dash, M. Yousufuddin, M. A. Celik, G. Frenking, *Inorg. Chem.* **2011**, *50*, 4253–4255; b) C. Dash, P. Kroll, M. Yousufuddin, H. V. R. Dias, *Chem. Commun.* **2011**, 47, 4478–4480. This is all in accordance with expected values for non-classical carbonyls; c) P. K. Hurlburt, J. J. Rack, J. S. Luck, S. F. Dec, J. D. Webb, O. P. Anderson, S. H. Strauss, *J. Am. Chem. Soc.* **1994**, *116*, 10003–10014.
- [21] T. N. Hooper, M. Green, C. A. Russell, *Chem. Commun.* **2010**, 46, 2313–2315.
- [22] gNMR V5 Adept Scientific Plc **2003**.
- [23] R. M. Lynden-Bell, N. Sheppard, *Proc. Roy. Soc. London Ser. A.* **1962**, *269*, 385.
- [24] Y. N. Luzikov, N. M. Sergeyev, *J. Magn. Reson.* **1984**, *60*, 177–183.
- [25] Related slightly larger $1J(\text{CH})$ values than free olefin have been reported in d10 ethylene complexes. See for example a) B. F. Straub, F. E. P. Hofmann, *Chem. Commun.* **1999**, 2507–2508; b) B. T. Watson, M. Vanga, A. Noonikara-Poyil, A. Muñoz-Castro, H. V. R. Dias, *Inorg. Chem.* **2023**, *62*, 1636–1648.
- [26] J. Krause, W. Bonrath, K. R. Poerschke, *Organometallics* **1992**, *11*, 1158–1167.
- [27] This stability in the solid-state suggests that exchange processes may be associative, and in solution anions or solvent may provide alternative—deleterious—pathways that are not accessible in the single-crystal.
- [28] a) S. H. Lim, M. M. Olmstead, A. L. Balch, *Chem. Sci.* **2013**, *4*, 311–318; b) N. K. Sethi, A. C. Whitwood, D. W. Bruce, *Inorg. Chem.* **2018**, *57*, 13524–13532.
- [29] a) E. V. Patrick, M. E. Bowden, J. D. Erickson, R. M. Bullock, B. L. Tran, *Angew. Chem. Int. Ed.* **2023**, *62*, e202304648; b) H. V. R. Dias, D. Parasar, A. A. Yakovenko, P. W. Stephens, A. Muñoz-Castro, M. Vanga, P. Mykhailiuk, E. Slabodyanyuk, *Chem. Sci.* **2024**, *15*, 2019–2025.
- [30] H. Fast, H. L. Welsh, *J. Mol. Spectrosc.* **1972**, *41*, 203–221.
- [31] M. S. Nechaev, V. M. Ravón, G. Frenking, *J. Phys. Chem. A.* **2004**, *108*, 3134–3142.

Manuscript received: March 1, 2024

Accepted manuscript online: May 3, 2024

Version of record online: ■■■■■

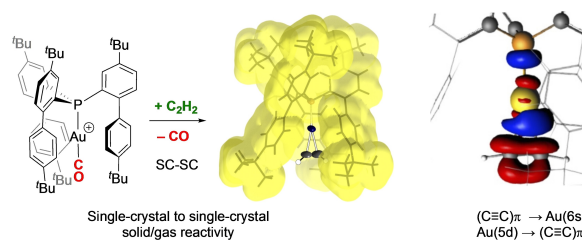
Communications

Gold Chemistry

C. L. Johnson, D. J. Storm, M. A. Sajjad,
M. R. Gyton, S. B. Duckett,*
S. A. Macgregor,* A. S. Weller,*
M. Navarro,* J. Campos* — e202404264

A Gold(I)–Acetylene Complex Synthesised
using Single-Crystal Reactivity

Synthesis and characterization of a gold(I)acetylene complex using *in crystallo* methods



The existence of π -acetylene gold(I) compounds as intermediates in catalysis has been postulated, but their isolation or spectroscopic detection has remained elusive. Herein, the combination of a bulky cavity-shaped phosphine along with single-crystal to single-crystal reac-

tivity allowed for the isolation of the first gold(I)–acetylene complex, which was thoroughly characterized by X-ray diffraction, solution and solid-state NMR, periodic DFT, and electronic structure analyses.



@Miquelnb @CamposGroup @WellerYorkChem

Share your work on social media! *Angewandte Chemie* has added Twitter as a means to promote your article. Twitter is an online microblogging service that enables its users to send and read short messages and media, known as tweets. Please check the pre-written tweet in the galley proofs for accuracy. If you, your team, or institution have a Twitter account, please include its handle @username. Please use hashtags only for the most important keywords, such as #catalysis, #nanoparticles, or #proteindesign. The ToC picture and a link to your article will be added automatically, so the **tweet text must not exceed 250 characters**. This tweet will be posted on the journal's Twitter account (follow us @angew_chem) upon publication of your article in its final (possibly unpaginated) form. We recommend you to re-tweet it to alert more researchers about your publication, or to point it out to your institution's social media team.

Please check that the ORCID identifiers listed below are correct. We encourage all authors to provide an ORCID identifier for each coauthor. ORCID is a registry that provides researchers with a unique digital identifier. Some funding agencies recommend or even require the inclusion of ORCID IDs in all published articles, and authors should consult their funding agency guidelines for details. Registration is easy and free; for further information, see <http://orcid.org/>.

Daniel J. Storm

Prof. Simon B. Duckett <http://orcid.org/0000-0001-8378-8793>

Prof. Andrew S. Weller <http://orcid.org/0000-0003-1646-8081>

Dr. Matthew R. Gyton <http://orcid.org/0000-0002-7565-5154>

Dr. Miquel Navarro <http://orcid.org/0000-0002-5481-1234>

Chloe L. Johnson

Dr. M. Arif Sajjad <http://orcid.org/0000-0002-4119-9912>

Dr. Jesús Campos <http://orcid.org/0000-0002-5155-1262>

Prof. Stuart A. Macgregor <http://orcid.org/0000-0003-3454-6776>